Inflammation, Vol. 42, No. 2, April 2019 (© 2018)
DOI: 10.1007/s10753-018-0914-4

ORIGINAL ARTICLE

Neuronal EphA4 Regulates OGD/R-Induced Apoptosis by Promoting Alternative Activation of Microglia

Hui-Xing Wei,[1] Pei-Sen Yao,[2] Ping-Ping Chen,[1] Jian-Hua Guan,[1] Jin-Hong Zhuang,[1] Jia-Bin Zhu,[1,3] Gang Wu,[1,4] and Jin-Shan Yang[1,4]

Abstract— Accumulating evidence indicates that post-injury inflammation characterized by activated microglia contributes much to the neuropathology of ischemic injury. Several studies have demonstrated that microglia exhibit two entirely different functional activation states, referred to as classically activated (M1) and alternatively activated (M2) phenotype. Promoting microglial phenotype to switch from M1 dominant to M2 dominant might be a promising approach for handling ischemic injury. However, the comprehensive mechanism that underlines microglia polarization in ischemic brain remains unclear. Neuronal erythropoietin-producing human hepatocellular carcinoma cell receptor 4 (EphA4), the richest Eph receptor in the central nervous system (CNS), upregulate after ischemia and may have the potential to regulate microglia activation. We hypothesized that modulating EphA4/ephrin signaling could affect ischemic injury through controlling microglia polarization. We therefore knocked down neuronal EphA4 with short hairpin RNA (shRNA) and determined the role of EphA4/ephrin signaling in oxygen-glucose deprivation and reperfusion (OGD/R)-induced injury. We found that EphA4 shRNA treatment attenuated OGD/R-induced apoptosis and microglia proliferation. Neuronal EphA4 knockdown also promoted microglial M2 polarization, which reduced pro-inflammatory mediators and released anti-inflammatory cytokines as well as neurotrophic factors. We further revealed that EphA4 shRNA treatment functioned through RhoA/Rho-associated kinase 2 (ROCK2) signaling, a key mediator of microglia

Hui-Xing Wei and Pei-Sen Yao contributed equally to this work.

Electronic supplementary material The online version of this article (https://doi.org/10.1007/s10753-018-0914-4) contains supplementary material, which is available to authorized users.

[1] Department of Neurology, The First Affiliated Hospital of Fujian Medical University, 20 Chazhong Road, Fuzhou, 350000, Fujian, People's Republic of China
[2] Department of Neurosurgery, The First Affiliated Hospital of Fujian Medical University, Fuzhou, People's Republic of China
[3] Department of Neurology, Huian County Hospital, Quanzhou, People's Republic of China
[4] To whom correspondence should be addressed at Department of Neurology, The First Affiliated Hospital of Fujian Medical University, 20 Chazhong Road, Fuzhou, 350000, Fujian, People's Republic of China. E-mails: gangwu444@sina.com; jinshan_yang@sina.com

alternative activation. Together, these data suggested that blockage of EphA4/ephrin signaling between neuron and microglia decreased OGD/R-induced injury by promoting alternative activation of microglia *via* RhoA/ROCK2 signaling.

KEY WORDS: Ischemia; inflammatory injury; EphA4/ephrin signaling; microglial polarization; RhoA/ROCK2 signaling.

INTRODUCTION

Post-injury inflammation, which is characterized by microglial activation and circulating immune cell infiltration in the brain, plays a critical role during the pathological process of ischemia. Microglia, as brain resident macrophage, represent the first line of defense against brain injuries such as ischemia. Activated microglia accumulate at the border zone of injury and exhibit double-edged sword effect in neurological recovery. On the one hand, activated microglia can amplify the ischemic lesion through producing pro-inflammatory mediators and toxic molecules, but on the other hand, microglia may also set the stage for tissue remodeling by clearing cellular debris and release neurotrophic factors [20].

Different polarization of microglia could likely explain the biphasic role of microglia after brain injury. The classical M1 phenotype, also known as inflammatory phenotype, is characterized by the production of a variety of pro-inflammatory cytokines. On contrast, the alternative M2 phenotype contributes to inhibiting inflammation and promoting tissue repair through expressing scavenge receptors, as well as producing anti-inflammatory cytokines and neurotrophic factors [3]. Promoting alternative activation of microglia, switching phenotype from M1 dominant to M2 dominant, might be a promising approach for handling ischemic injury [13]. Microglia polarization is a comprehensive process that can be affected by surrounding cells such as neurons. The interaction between neuron and microglia is complicated and found to be involved in microglia polarization [14].

Eph proteins constitute the largest known receptor tyrosine kinase family. Eph receptors are activated when bound to membrane-combined ephrin ligands. The formation of the Eph/ephrin complex initiates bidirectional signaling, which acts upon both Eph-expressing and ephrin-expressing cells at the same time [37]. EphA4, the most abundantly expressed Eph receptor in the central nervous system (CNS), is mainly distributed in neurons [2, 8, 23]. Our previous study showed that EphA4 upregulated and was involved in the pathological process of ischemic brain injury [36]. Furthermore, EphA4/ephrin signaling may also function through microglia and regulate inflammatory injury after ischemia [15, 26, 35], but the specific mechanism remains unclear.

In this paper, we aim to determine the role played by EphA4/ephrin signaling between neuron and microglia in ischemic inflammatory injury. The EphA4 shRNA was applied to manipulate EphA4/ephrin signaling. The role of EphA4/ephrin signaling in ischemic injury was investigated *in vitro* by detecting changes in neuron damage, microglial alternative activation, and RhoA/ ROCK2 signaling. Our results showed that blockage of EphA4/ephrin signaling between neuron and microglia decreased OGD/R-induced apoptosis through promoting microglia M2 polarization *via* RhoA/ROCK2 signaling.

MATERIALS AND METHODS

EphA4 shRNA Lentiviral Vectors Construction and Neuronal Infection

Three candidate sequences were designed basing on the mouse EphA4 mRNA gene sequence (NM_007936.3) in the GenBank database (http://www.ncbi.nlm.nih.gov/genbank/) according to shRNA design principles [5]. The EphA4 shRNA template oligonucleotides were cloned into the pGreenPuro vector (System Biosciences) in accordance with the manufacturer's protocol. Positive clones carrying the target shRNA template were identified by real-time reverse transcription-polymerase chain reaction (RT-PCR). The positive plasmid was then transformed into *Escherichia coli* DH5α competent cells (TransGen Biotech) for plasmid amplification. For lentivirus production, plasmids containing the EphA4 shRNA template were transfected into 293T cells (System Biosciences) using Lipofectamine 3000 (Invitrogen). Primary neurons were infected (viral titer 2×10^8 TU/ml) at day *in vitro* (DIV) 2 for 24 h at 37 °C. Cultures were incubated in normal culture medium for a further 2 days before further experiments [12]. The transfected cells were identified by green fluorescent protein (GFP) staining. The silencing efficiency of different EphA4 shRNA was estimated by

determining the concentration of target mRNA using RT-PCR as well as assessing the amount of target protein by Western blot. The two more efficient silencing sequences of EphA4 shRNA were selected for subsequent studies. The sequence 5′-TTCTCCGAACGTGTCACGT-3′ was used as nonspecific negative control.

Hippocampal Neuronal Culture

All animal experiments were performed in accordance with the guidelines for the animal care and use of laboratory animal protocols approved by the international guidelines for the ethical use of laboratory animals and the Institutional Animal Care and Use Committee at Fujian Medical University.

Hippocampal neurons were obtained from C57BL/6 mice as described before [39]. Briefly, both hippocampi of P0 mouse were dissected and dissociated with 0.125% trypsin (Invitrogen), and then cells were plated in poly-L-lysine (Sigma) coated 96-well plate (5×10^4 cells/well) or 24-well plate (10^5 cells/well) with neurobasal medium containing 2% B27 (Gibco) supplement, 1% antibiotic-antifungal mixture, and 0.5 mM L-glutamine (Sigma). A double immunofluorescence staining of anti-microtubule associated protein-2 (MAP-2) (1:200, Abcam, Cat. No. ab96378, RRID: AB_10678243) and 2-(4-Amidinophenyl)-6-indolecarbamidine dihydrochloride (DAPI) (1 g/ml, Sigma) was used to determine the purity of primary neurons, cultures of more than 95% purity were used for further experiments.

Primary Culture of Microglia

Microglia were isolated from mixed glial cultures according to the method described previously with slight modifications [10]. Briefly, the cerebral cortices of P0-P1 C57BL/6 mouse were dissociated and digested with 0.25% trypsin (5 min, 37 °C). The cells were seeded in 75 cm^2 poly-L-lysine-coated culture flasks and cultured with Dulbecco's modified Eagle's medium (DMEM)/F12 (1:1) containing 100 U/ml penicillin, 100 μg/ml streptomycin, and 10% fetal bovine serum (FBS). After being confluent cultured for 10 days, flasks were gently shaken by an orbital shaker (37 °C, 200 rpm, 1.5 h). The supernatant containing the microglia was collected, and the cells were then plated onto poly-L-lysine-coated glass coverslips at a density of 5×10^6 cells/cm^2. Thirty minutes later, the medium was refreshed, and microglia were isolated as strongly adherent cells. A double immunofluorescence staining of Iba-1 (1:400, Wako Pure Chemical Industries, Cat. No. 019-19741, RRID: AB_839504) and DAPI was used to determine the purity of microglia cultures. The results showed that more than 95% of the primary cultures were Iba-1-positive microglia.

Neuron-Microglia Coculture and OGD/R Treatment

Purified microglial cells were resuspended in neuronal medium and seeded into wells containing primary neurons at DIV 5 at a cell density of 2.5×10^4 cells/well (96-well plate) or 5×10^4 cells/well (24-well plate). To mimic the pathological process induced by ischemia *in vitro*, 3 h after plating, co-cultures were subjected to hypoxia treatment. In brief, co-cultures were cultured with serum and glucose-free DMEM in an anaerobic chamber (Thermo Fisher Scientific) containing 93% N_2, 5% CO_2, and 2% O_2 for 60 min. After OGD/R, the co-cultures were returned to neuron-conditioned medium and placed in a normoxic chamber (95% O_2 and 5% CO_2). Cells were collected 24 h after OGD/R intervention for subsequent experiments. Primary neurons in the sh-EphA4 group, OGD + Control shRNA group, and OGD + sh-EphA4 group were infected with EphA4 shRNA lentiviral vectors before coculture.

Quantitative Real-time PCR

Total RNA was extracted from cell cultures by using an RNeasy Mini kit (Qiagen). The reverse transcription reaction was carried out with a PrimeScript™ 1st strand cDNA Synthesis Kit (Takara) according to the manufacturer's protocol. PCR was carried out on ABI Prism7500 sequence detection system (Applied Biosystems) at 95 °C for 10 min, then 40 cycles at 95 °C for 10 s, at 58 °C for 30 s, and 30 s at 72 °C. Amplification of specific PCR products was detected using the SYBR Green PCR Master Mix (Takara) according to the manufacturer's protocol. Data were analyzed using a comparative 2-ΔΔ cycle threshold (CT) method with the glyceraldehyde 3-phosphate dehydrogenase (GAPDH) as an endogenous reference [19].

Western Blot Analysis

Western blot analysis was carried out to investigate changes of the protein expression of EphA4, proliferating cell nuclear antigen (PCNA), inducible nitric oxide synthase (iNOS), arginase 1 (Arg1), Ym1, RhoA, GTP-RhoA, and ROCK2. Briefly, cells were harvested and then homogenized by sonication in CHAPS lysis buffer (50 mM Tris-HCl pH 7.7, 150 mM NaCl, 1% CHAPS) with protease inhibitor

cocktail. Tissue lysates were centrifuged at 12000*g* at 4 °C for 10 min and then supernatants were carefully collected. Protein concentrations were determined using a bicinchoninic acid (BCA) protein quantitation kit (Boster) according to the manufacturer's protocol. Protein samples were loaded and run on a 12% polyacrylamide gel, and then proteins of specific molecular weight separated by electrophoresis were transferred to a nitrocellulose membrane (0.45 μm, Millipore) using a wet transfer system (Bio-Rad Laboratories). After blocking nonspecific binding sites with 5% non-fat milk (BD biosciences), 0.25% Tween-20 (Amresco) in Tris-buffered saline for 90 min at 20 to 25 °C, membranes were incubated with specific primary antibodies (anti-GAPDH, 1:500, Boster, Cat. No. BA2913, RRID: AB_2560936; anti-β-tubulin, 1:500, Abcam, Cat. No. ab6046, RRID: AB_2210370; anti-EphA4, 1:500, Abcam, Cat. No. ab5396, RRID: AB_304857; PCNA, 1:1000, Abcam, Cat. No. ab92552, RRID: AB_10561973; anti-iNOS, 1:400, Abcam, Cat. No. ab3523, RRID: AB_303872; anti-Arg1, 1:1000, Cell Signaling Technology, Cat. 9819; anti-Ym1, 1 μg/ml, Abcam, Cat. No. ab93034, RRID: AB_10863056; anti-RhoA, 1:1000, Abcam, Cat. No. ab86297, RRID: AB_10675086; anti-ROCK2, 1:5000, Abcam, Cat. No. ab125025, RRID: AB_10972853) at 4 °C on a rocker platform overnight. Then, membranes were incubated with the appropriate secondary antibodies which were anti-rabbit horseradish peroxidase-conjugated (1:5000, Santa Cruz Biotechnology, Cat. No. sc-2357, RRID: AB_628497). Finally, membranes were detected by an enhanced chemiluminescence (ECL) kit (Thermo Fisher Scientific) according to the manufacturer's protocol. The resulting digital images were analyzed by Image J to obtain the integrated optical density (OD) of signals. Either GAPDH or β-tubulin acted as an internal control to normalize the target protein expression.

Immunofluorescent Staining

To detect the cellular protein expressions, immunofluorescent staining was carried out. Briefly, the cell cultures were post-fixed in 100% ice-cold methanol for 15 min. After blocking nonspecific antibody binding site by 10% bovine serum albumin (BSA)/phosphate buffered saline (PBS), cell cultures were incubated with primary antibodies (anti-EphA4,1:400, Abcam, Cat. No. ab5396, RRID: AB_304857; anti-MAP-2, 1:200, Abcam, Cat. No. ab96378, RRID: AB_10678243; anti-Iba-1, 1:400, Wako Pure Chemical Industries, Cat. No. 019-19741, RRID: AB_839504; anti-ROCK2, 1:200, Abcam, Cat. No. ab125025, RRID: AB_10972853; anti-Iba-1, 1:400, Abcam, Cat. No. ab5076, RRID: AB_2224402) overnight at 4 °C. Then cultures were incubated with mixed secondary antibodies containing Cyanine 3 (CY3)-conjugated goat anti-rabbit IgG antibody (1:400, Jackson ImmunoResearch Laboratories, Cat. No. 111–165-003, RRID: AB_2338000) or fluorescein (FITC)-conjugated donkey anti-goat IgG antibody (1:200, Jackson ImmunoResearch Laboratories, Cat. No. 705–095-147, RRID: AB_2340401) for 1 h at 20 to 25 °C. After being washed three times in PBS for 5 min, the sections were dried and mounted, and then covered with a coverslip. Finally, the Olympus BX51 fluorescent microscope (Olympus) was used to observe the results of immunofluorescent staining. The average number of Iba-1-stained cells in four randomly chosen view fields out of each slide was counted for microglia number quantification.

Flow Cytometry Analysis for OGD/R-Induced Apoptosis

An Annexin V- Fluorescein Isothiocyanate (FITC) Early Apoptosis Detection Kit (Cell Signaling Technology) was used to detect early and late apoptotic cells according to the manufacturer's instructions. Briefly, cells were trypsinized and washed twice in ice-cold PBS. Then cells were resuspended at 1×10^6–5×10^6 cells/ml with 1× Annexin V Binding Buffer. A total of 96 μl cell suspension was added into an assay tube. A mixture of 1 μl Annexin V-FITC and 12.5 μl propidium iodide (PI) was added into the cell suspension, and after incubation for 10 min at room temperature in the dark, the samples were immediately analyzed by flow cytometry (Beckman FC 500). Early apoptotic cells with high Annexin V-FITC staining but low PI staining (Quadrant 3) and late apoptotic or necrotic cells with high Annexin V-FITC and PI staining (Quadrant 2) and necrotic cells with high PI staining but low Annexin V-FITC staining (Quadrant 1) were counted.

Enzyme-Linked Immunosorbent Assay

To detect the cytokine changes after treatment, cell supernatants of co-cultures were collected. The levels of IL-1β, IL-4, IL-6, IL-10, TNF-α, and TGF-β in the supernatant of neuron-microglia co-cultures were measured by using a sandwich ELISA kit (Invitrogen) according to the manufacturer's instructions. A standard reference curve was prepared for each assay for accurate quantitation of cytokine levels in samples.

Nitric Oxide Assay Kit

The concentration of nitric oxide (NO) was determined by measuring the amount of both nitrate and nitrite concentrations in the sample by using a NO assay kit (Invitrogen) according to the manufacturer's instructions. Briefly, the nitrate in the sample was converted into nitrite by nitrate reductase in the presence of nicotinamide adenine dinucleotide phosphate (NADPH). Nitrite was then converted into a chromophore compound based on the Griess reaction. After incubation with Griess reagent (1:1 ratio) at room temperature for 15 min, the absorbance at 540 nm was measured with a microplate reader (Bio-Rad Laboratories). Nitrite concentration was calculated with reference to a standard curve of sodium nitrite generated using known concentrations.

Activated RhoA Detection

GTP-Rho pull-down assays were performed to test RhoA activation using Rho Activation Assay Kit according to the supplier's protocol (Upstate/Millipore). Briefly, a total of 5×10^6 cell lysates from treated and control groups were incubated with the Rhotekin RBD-agarose slurry at 4 °C for 45 min with gentle agitation and then washed three times with wash buffer. The bound proteins were boiled and eluted with 2× sample buffer and detected by SDS-PAGE as described above.

Statistical Analysis

Statistical analyses were processed by SPSS 19.0 (SPSS Inc.). All data were expressed as the mean ± SD and evaluated by one-way analysis of variance (ANOVA) followed by Tukey's *post hoc* test to compare differences between groups. Statistical significance was considered at a value of $P < 0.05$.

RESULTS

EphA4 shRNA Lentiviral Vectors Construction and Selection

Primers for the designed EphA4-specific shRNAs and control shRNA were shown in Fig. 1b. The silencing efficiency of EphA4 shRNA is shown in Fig. 1c–e. The screening results showed that all three EphA4 shRNAs exhibited significant silencing effect on the EphA4 mRNA expression levels than those of the control group ($P < 0.01$) (Fig. 1c), with the higher inhibition rate in the EphA4 shRNA-1(84.68%) and EphA4 shRNA-3 group (93.56%). Similarly, the expression levels of EphA4 protein in all the three shRNA groups were significantly lower than those of the control group ($P < 0.01$) (Fig. 1d, e). The EphA4 shRNA-1 and EphA4 shRNA-3 also showed more significant silencing effect (75.29% and 80.21%, respectively), and were selected for subsequent studies. In the sh-EphA4 group, neuronal EphA4 was knocked down by EphA4 shRNA-3 before coculture to evaluate the effects of EphA4 at baseline. Co-staining of GFP and Iba1 confirmed that microglia in co-cultures were not infected by EphA4 shRNA lentivirus (Fig. S1).

EphA4 Cellular Expression

The cellular distribution of EphA4 receptor was investigated by immunofluorescent staining. As revealed in Fig. 1a, EphA4 receptor was found to be expressed in the hippocampal neuronal culture. This was consistent with our previous study *in vivo* which had confirmed the specific cellular distribution of the EphA4 receptor in NeuN-positive pyramidal neurons throughout the hippocampus [36].

EphA4 shRNA Decreased OGD/R-Induced Apoptosis and Microglia Proliferation

To investigate the EphA4/ephrin signaling between neuron and microglia, we used shRNA to knockdown neuronal EphA4. As shown in Fig. 2a, b, both EphA4 shRNA-1 and EphA4 shRNA-3 application significantly decreased OGD/R-induced early apoptosis as well as late apoptosis and necrosis which were confirmed by flow cytometry analysis ($P < 0.01$). Immunocytochemical staining with Iba1 showed that EphA4 shRNA treatment also inhibited the microglia proliferation and activation induced by OGD/R. In both two EphA4 shRNA-treated groups, microglia in the co-cultures were lesser, smaller, and less irregularly shaped than OGD and control shRNA-treated group (Fig. 2c, d). We also found that PCNA protein expressions, which upregulated after OGD, decreased significantly in both EphA4 shRNA-treated groups (Fig. 2e, f). This suggests that application of EphA4 shRNA decreased neuronal apoptosis as well as microglia proliferation and activation.

Effects of EphA4 shRNA on Alternative Activation of Microglia

As the morphological change could not always precisely reflect the microglia activation states, we further investigated the influence of EphA4 shRNA on

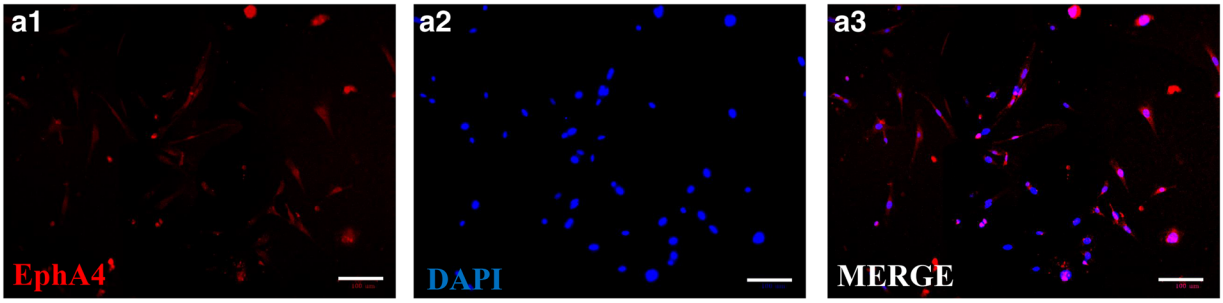

b

shRNA	Sequence (5′-3′)
shRNA-1	Sense: GATCCGCACCATCATCCATTGCTTTGCTCGAGCAAAGCAATGGATGATGGTGCTTTTTG
	Antisense: AATTCAAAAAGCACCATCATCCATTGCTTTGCTCGAGCAAAGCAATGGATGATGGTGCG
shRNA-2	Sense: GATCCGGTCCAGGCTAAAGAAGTTACCTCGAGGTAACTTCTTTAGCCTGGACCTTTTTG
	Antisense: AATTCAAAAAGGTCCAGGCTAAAGAAGTTACCTCGAGGTAACTTCTTTAGCCTGGACCG
shRNA-3	Sense: GATCCGGAAGAATGATGGCCGCTTTACTCGAGTAAAGCGGCCATCATTCTTCCTTTTTG
	Antisense: AATTCAAAAAGGAAGAATGATGGCCGCTTTACTCGAGTAAAGCGGCCATCATTCTTCCG
Control shRNA	Sense: TTCTCCGAACGTGTCACGT

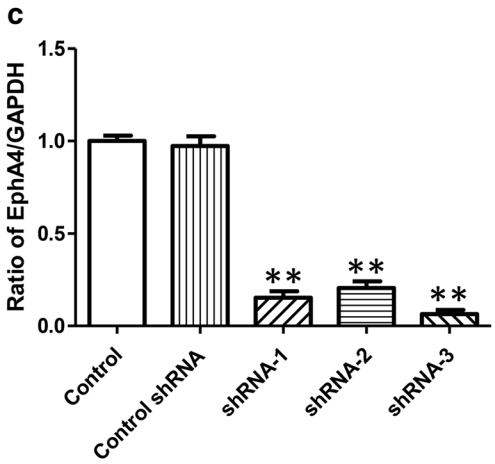

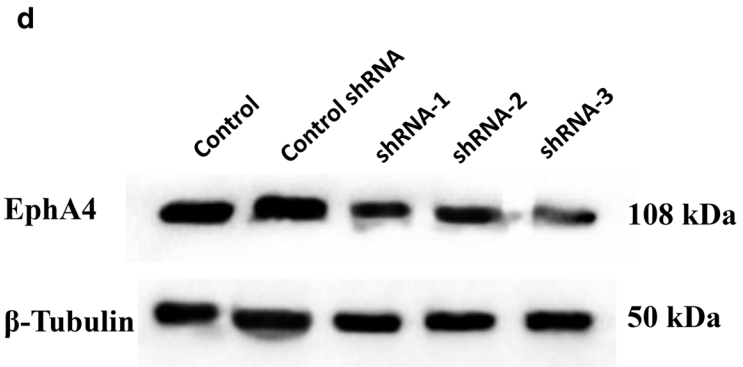

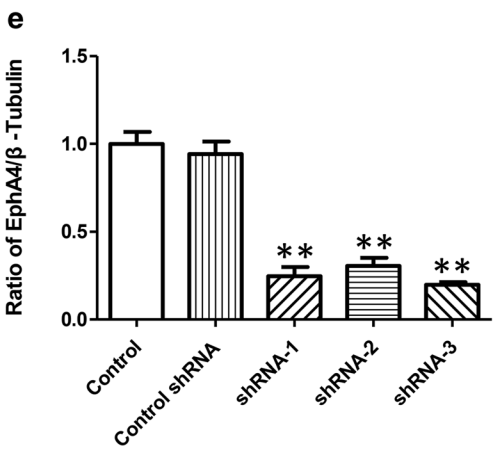

Fig. 1. Construction of lentiviral vectors expressing EphA4 shRNAs. **a** Expression of EphA4 on neurons identified by staining with anti-EphA4 antibody (red) and DAPI (blue). Scale bar = 100 μm. **b** Primers for the designed EphA4-specific shRNAs and control shRNA. c The introduction of the EphA4-specific shRNAs reduced the level of the EphA4 mRNA, as assessed by real-time PCR. EphA4 mRNA expression was normalized to GAPDH and quantified. **d** The level of the EphA4 protein was assessed by Western blot. **e** Quantification of EphA4 protein levels. All three EphA4 shRNAs exhibited significant silencing effect on the EphA4 protein expression levels than those of the control group. Protein expression was normalized to β-tubulin. The results were presented as the means ± SD, and data were evaluated using one-way ANOVA and Tukey's *post hoc* test ($n = 5$ samples per group, $^{**}P < 0.01$ compared with the control group).

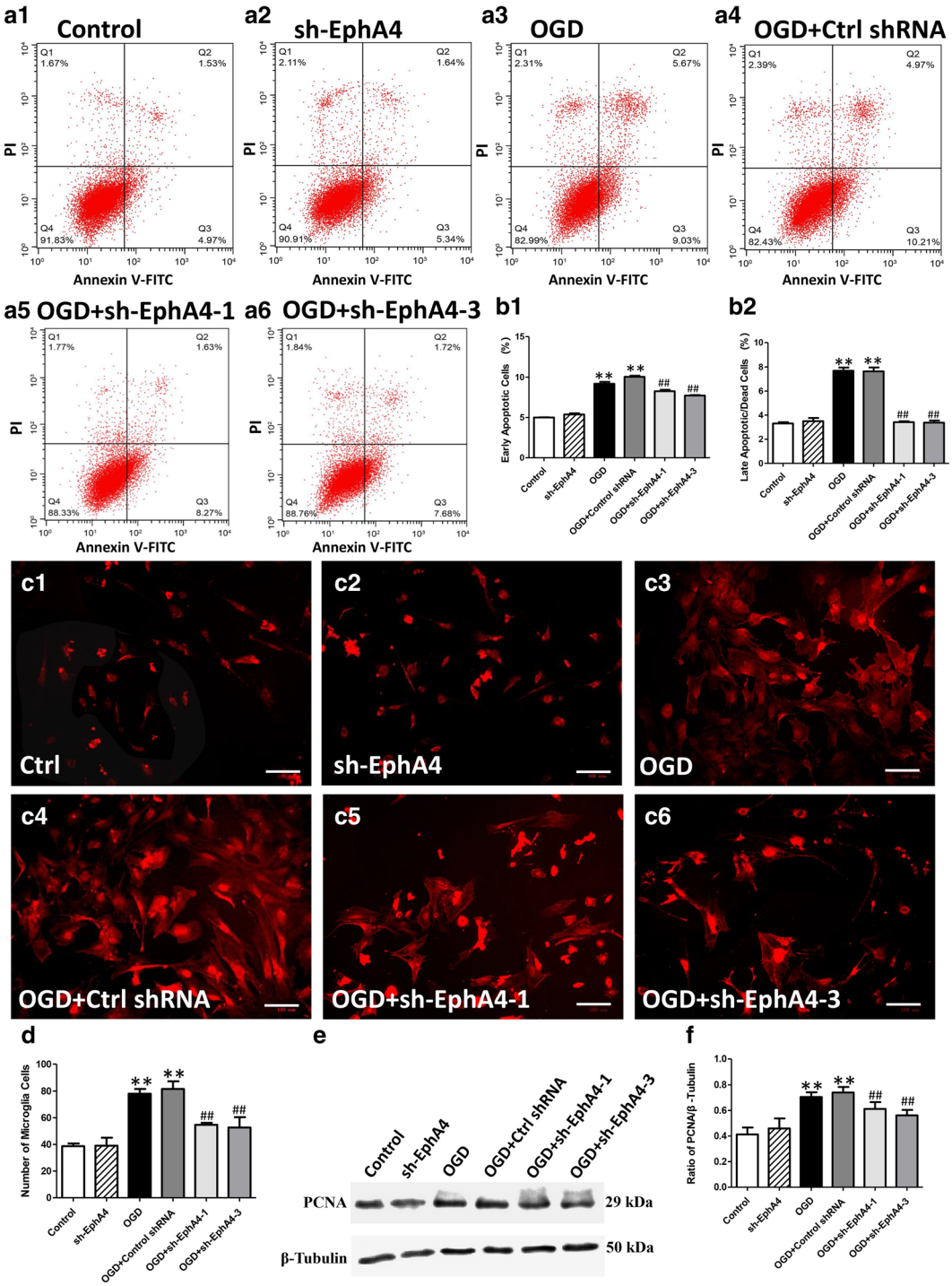

Fig. 2. The application of the EphA4-specific shRNA reduced neuronal apoptosis and microglial proliferation. **a** Representative examples of flow cytometry data showing the percentages of apoptotic cells. **b** The flow cytometry data indicated the percentage of apoptotic cells in each group. **c** The number and morphology of primary microglia in co-cultures changed in response to the treatment. Microglia were stained with Iba1 (red). **d** Quantification of microglia number. **e** The protein level of PCNA was assessed by Western blot. **f** Quantification of PCNA protein levels. Protein expression was normalized to β-tubulin. The results were presented as the means ± SD, and data were evaluated using one-way ANOVA and Tukey's *post hoc* test ($n = 5$ samples per group, $^{**}P < 0.01$ compared with the control group; $^{\#\#}P < 0.01$ compared with the OGD group).

microglia-activation states by determining the levels of the key microglial enzymes, iNOS, Arg1, and Ym1, which are the best characterized molecule markers of the M1 (iNOS) and M2 (Arg1 and Ym1) phenotypes, respectively [3, 4, 21]. With EphA4 shRNA application prior to OGD/R, downregulation of iNOS ($P < 0.01$) and upregulation of Arg1 and Ym1 ($P < 0.01$) were determined at mRNA levels by using quantitative RT-PCR (Fig. 3a–d). As shown in Fig. 3e, f, Western blotting revealed that iNOS protein levels increased after OGD/R ($P < 0.01$) but decreased with EphA4 shRNA treatment ($P < 0.01$). We further analyzed Arg1 and Ym1 as markers for microglia alternative activation. On the contrary, Arg1 and Ym1 protein levels decreased slightly after OGD/R ($P < 0.05$) but increased significantly with EphA4 shRNA treatment ($P < 0.01$) (Fig. 3g–j). These results implicated that neuronal EphA4 knockdown converted microglia activation from classically activated states (M1) to alternative activated (M2) states. To investigate secretory function of microglia, levels of cytokines were further tested by ELISA kit. The secretion of the pro-inflammatory cytokines IL-1β, IL-6, and TNF-α, which increased significantly after OGD/R (IL-1β: 83.64 ± 1.74 pg/ml *vs* 64.57 ± 3.10 pg/ml, $P < 0.01$; IL-6: 140.46 ± 6.03 pg/ml *vs* 117.33 ± 4.07 pg/ml, $P < 0.01$; TNF-α: 367.09 ± 6.52 pg/ml *vs* 281.43 ± 7.61 pg/ml, $P < 0.01$), were inhibited by both EphA4-1 and EphA4 shRNA-3 shRNA treatment (IL-1β: 83.64 ± 1.74 pg/ml *vs* 72.15 ± 3.22 pg/ml, $P < 0.01$/ 66.82 ± 2.11 pg/ml, $P < 0.01$; IL-6: 140.46 ± 6.03 pg/ml *vs* 125.49 ± 5.08 pg/ml, $P < 0.05$/121.27 ± 7.07 pg/ml, $P < 0.05$; TNF-α: 367.09 ± 6.52 pg/ml *vs* 322.33 ± 11.94 pg/ml, $P < 0.01$/ 310.67 ± 11.62 pg/ml, $P < 0.01$) (Fig. 4a–c). Moreover, anti-inflammatory cytokines IL-4, IL-10, and TGF-β also increased significantly after OGD/R (IL-4: 373.81 ± 4.17 pg/ml *vs* 218.45 ± 13.31 pg/ml, $P < 0.01$; IL-10: 87.63 ± 3.58 pg/ml *vs* 70.31 ± 2.09 pg/ml, $P < 0.01$; TGF-β: 387.51 ± 19.83 pg/ml *vs* 220.78 ± 7.21 pg/ml, $P < 0.01$). With EphA4 shRNA-1 or EphA4 shRNA-3 treatment prior to OGD/R, IL-4 and TGF-β levels were significantly higher than OGD group (IL-4: 405.43 ± 8.02 pg/ml or 418.76 ± 23.02 pg/ml *vs* 373.81 ± 4.17 pg/ml, $P < 0.05$; TGF-β: 465.65 ± 14.30 pg/ml or 484.09 ± 20.06 pg/ml *vs* 387.51 ± 19.83 pg/ml, $P < 0.01$). The IL-10 level between two EphA4 shRNA-treated groups and ODG group showed no significance (88.55 ± 0.98 pg/ml *vs* 87.63 ± 3.58 pg/ml, $P = 0.688$; 90.34 ± 3.92 *vs* 87.63 ± 3.58 pg/ml, $P = 0.425$) (Fig. 4d–f). NO assay revealed that NO level in the culture medium increased after OGD/R (57.06 ± 3.09 μmol/L *vs* 23.92 ± 1.88 μmol/L, $P < 0.01$) but decreased with both EphA4 shRNA-1 and EphA4 shRNA-3 treatment (38.05 ± 2.08 μmol/L *vs* 57.06 ± 3.09 μmol/L, $P < 0.01$; 33.72 ± 4.70 μmol/L *vs* 57.06 ± 3.09 μmol/L, $P < 0.01$) (Fig. 4g). These findings indicated the involvement of EphA4/ephrin signaling between neuron and microglia in alternative activation of microglia.

Involvement of the RhoA/ROCK2 Signaling in EphA4 shRNA-Induced Changes in Alternative Activation of Microglia

Previous studies have identified the link between EphA/ephrin signaling and RhoA as well as its downstream effector ROCK. ROCK2 is highly expressed in the brain, while ROCK1 expression is negligible. Several lines of evidence have implicated that RhoA/ROCK2 play an essential role in control of microglial morphology and secretory function. In this study, we investigated whether EphA4 shRNA regulated the alternative activation of microglia *via* RhoA/ROCK2 signaling. Double immunofluorescent staining of ROCK2 and Iba-1 indicated that ROCK2 was highly expressed in cultured microglia (Fig. 5a). GTP-Rho pull-down assays were performed to assess the activation of RhoA. Upregulation of RhoA ($P < 0.05$), GTP-RhoA ($P < 0.01$), and ROCK2 ($P < 0.01$) protein expressions was observed after OGD/R. However, application of EphA4 shRNA prior to OGD/R inhibited RhoA, GTP-RhoA, and ROCK2 upregulation induced by OGD/R ($P < 0.01$) (Fig. 5b–e). Collectively, the above findings indicated that the RhoA/ROCK2 signaling pathway plays an important role in EphA4 shRNA-induced changes in alternative activation of microglia.

DISCUSSION

EphA4, the most abundantly expressed Eph receptor in the CNS, was mainly distributed in various neuronal populations throughout adult rodent and human brains [2, 8, 23, 37]. Our previous study revealed that neuronal EphA4 upregulated and affected ischemic brain injury through controlling astroglial glutamate uptake capacity [36]. Nevertheless, its role in microglial function and the possible mechanism remain poorly understood. In the present study, our results revealed that EphA4/ephrin signaling could also function through microglia to regulate ischemic injury. Here, we found that silencing neuronal EphA4 reduced inflammatory injury through shifting M1-state microglia to the M2-state *via* RhoA/ROCK2 signaling after OGD/R.

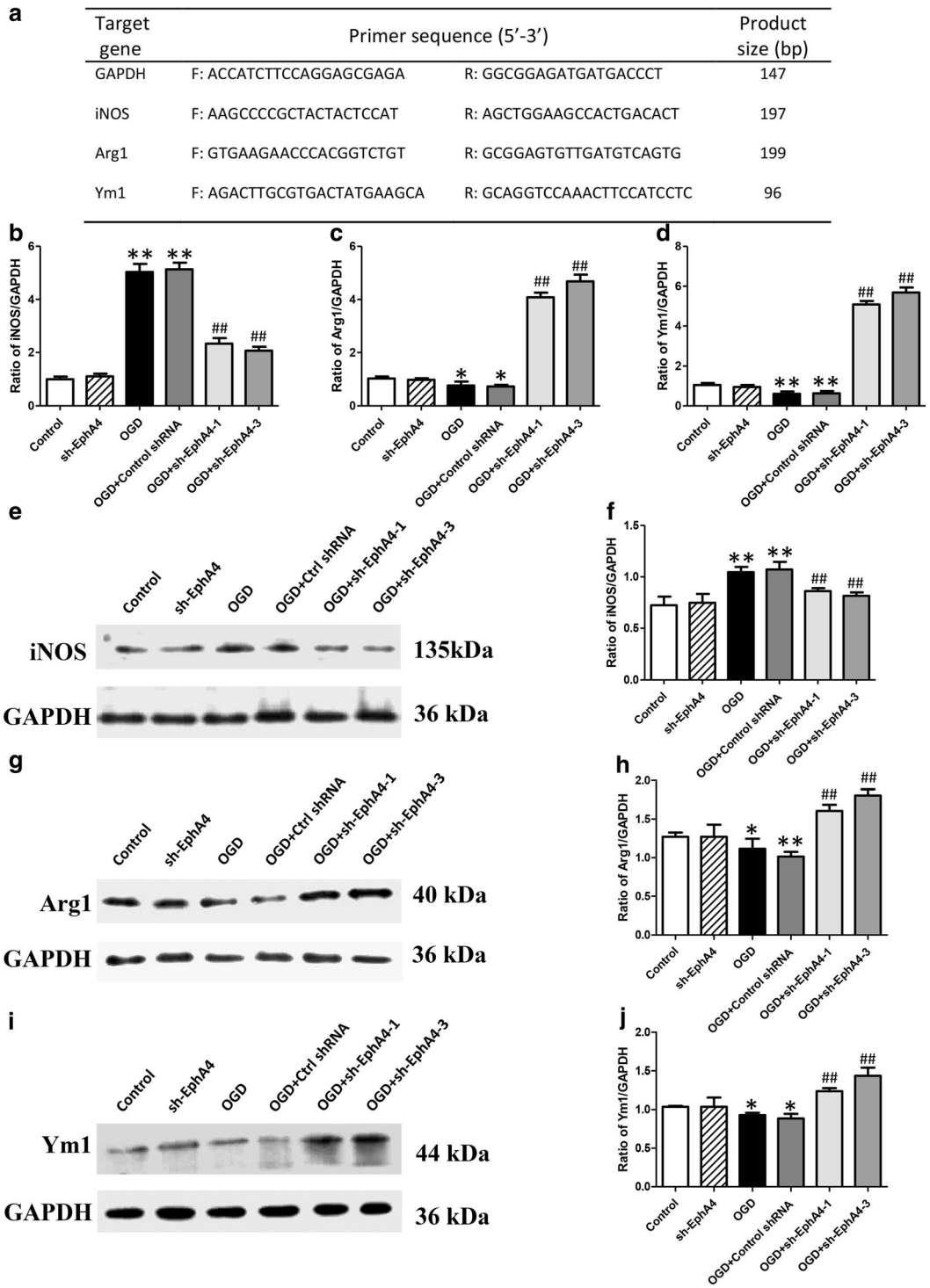

Fig. 3. Effects of neuronal EphA4 knockdown on the alternative activation of microglia. **a** Primers used for RT-PCR. **b**, **c**, **d** Quantitative RT-PCR of the mRNA levels of the iNOS (**b**), Arg1 (**c**), and Ym1(**d**) after OGD/R in cells treated with or without the EphA4 shRNA. **e**, **g**, **i** Western blot revealed changes in the protein levels of the iNOS (**e**), Arg1 (**g**), and Ym1 (**i**). **f**, **h**, **j** Quantification of the protein levels of the iNOS (**f**), Arg1 (**h**), and Ym1 (**j**). GAPDH was used as an internal standard to determine the protein level in each sample. The results were presented as the means ± SD, and data were evaluated using one-way ANOVA and Tukey's *post hoc* test ($n = 5$ samples per group, $^{*}P < 0.05$ and $^{**}P < 0.01$ compared with the control group; $^{\#\#}P < 0.01$ *vs* OGD group).

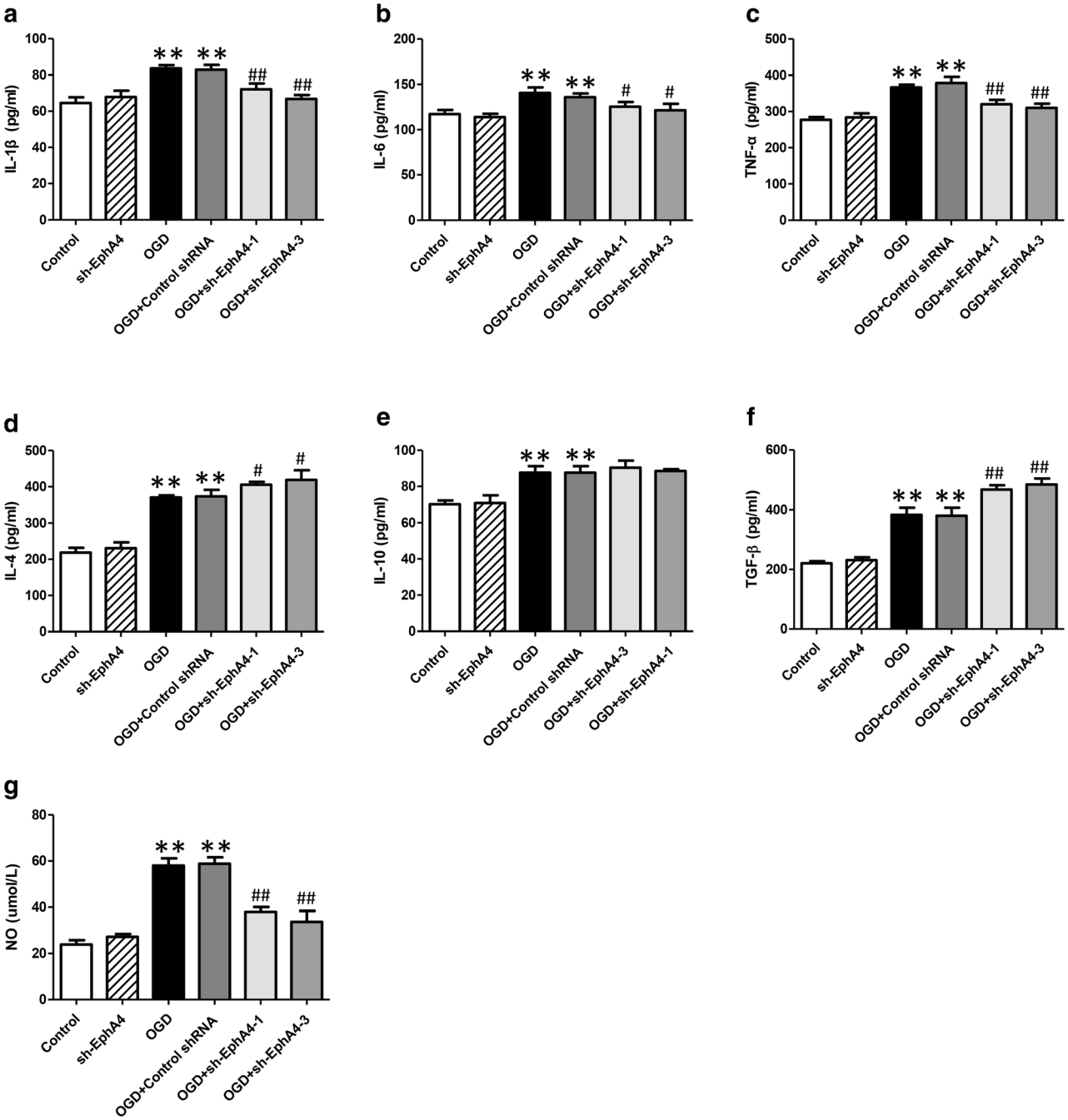

Fig. 4. Alterations in cytokine and NO concentrations after treatment. Neuronal EphA4 was knocked down with the EphA4 shRNAs or control shRNA prior to OGD/R, and then the concentrations of IL-1β (**a**), IL-6 (**b**), TNF-α (**c**), IL-4 (**d**), IL-10 (**e**), and TGF-β (**f**) were assessed using ELISA. The concentration of NO (**g**) was determined using a NO assay kit. The results were presented as the means ± SD, and data were evaluated using one-way ANOVA and Tukey's *post hoc* test ($n = 5$ samples per group, $^{**}P < 0.01$ compared with the control group; $^{\#}P < 0.05$ and $^{\#\#}P < 0.01$ compared with the OGD group).

Previous studies have validated that the bidirectional signaling existed between EphA4 receptor and ephrin ligands is involved in a series of neurological dysfunctions including ischemia [6, 7, 9, 31, 32]. Accumulating evidence suggests that EphA4 gene and protein expressions upregulated after ischemia, and inhibition of EphA4 has

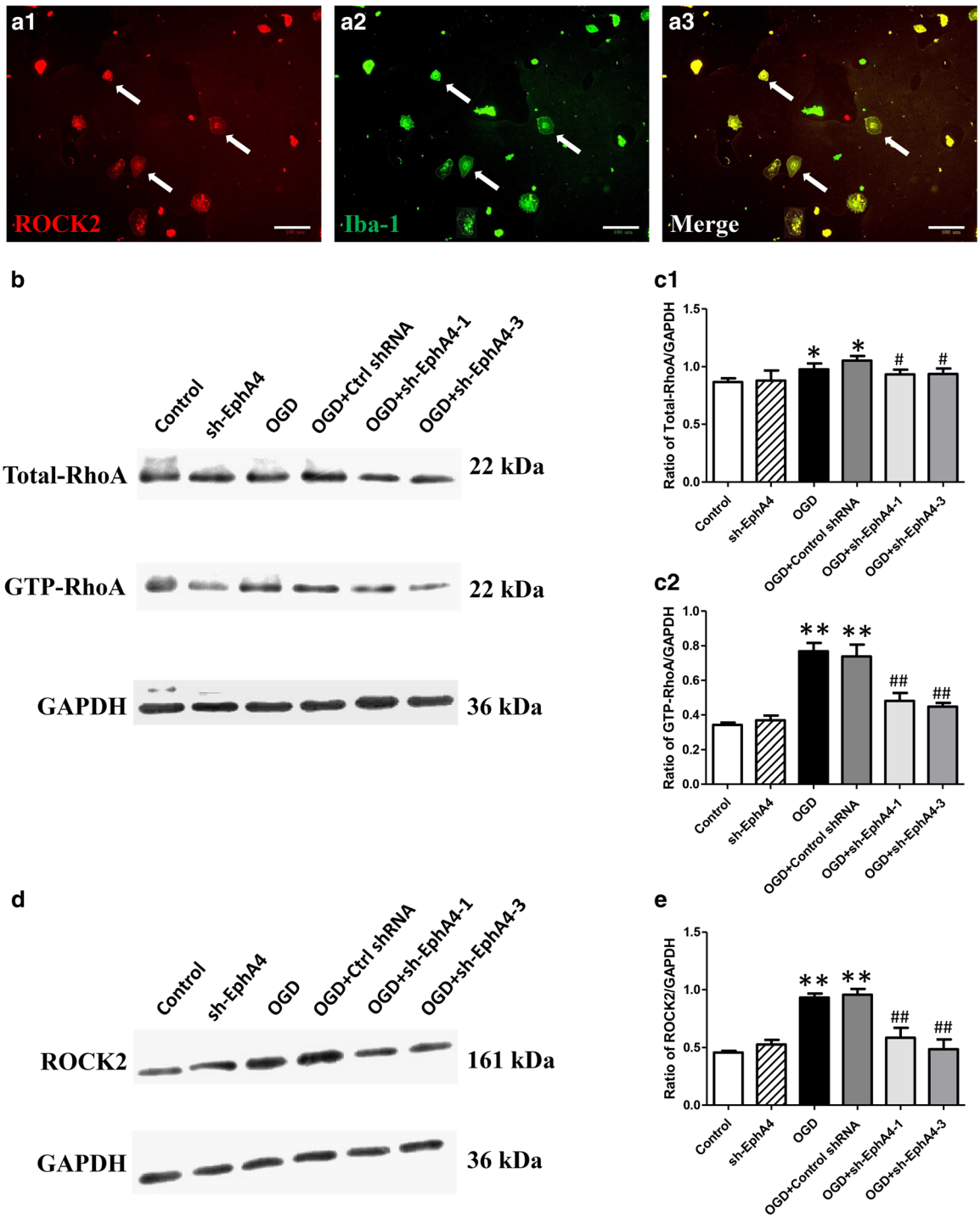

Fig. 5. Effects of the EphA4 shRNA on RhoA/ROCK2 signaling. **a** Expression of ROCK2 on microglia identified by staining with anti-ROCK2 antibody (red) and Iba-1 (green). Scale bar = 100 μm. **b**, **d** Representative Western blots showing the changes in the levels of the RhoA, activated RhoA (GTP-RhoA), and ROCK2 proteins in response to the EphA4 shRNA treatment after OGD/R. **c**, **e** Quantification of the levels of the RhoA, GTP-RhoA, and ROCK2 proteins. Protein expression was normalized to GAPDH. The results were presented as the means ± SD, and data were evaluated using one-way ANOVA and Tukey's *post hoc* test ($n = 5$ samples per group, $^{*}P < 0.05$ and $^{**}P < 0.01$ compared with the control group; $^{\#}P < 0.05$ and $^{\#\#}P < 0.01$ compared with the OGD group).

been shown to play protective role in ischemic injury [17, 18]. However, the precise mechanism of EphA4/ephrin signaling in regulating ischemic brain injury remains controversial and requires further investigation. Recent study has implicated that EphA4 is involved in the inflammatory response following spinal cord injury [22]. Consistent with these findings, our results showed that neuronal EphA4 appeared to be instrumental for the modulation of the microglial phenotype. Application of EphA4 shRNA to silence neuronal EphA4 resulted in decreased neuronal apoptosis through shifting microglia from M1-phenotype to M2-phenotype, and provided a rather neuroprotective environment by reducing pro-inflammatory cytokines (*e.g.*, IL-1, IL-6, TNF-α) as well as releasing anti-inflammatory mediators (*e.g.*, IL-4, TGF-β).

Both the Eph receptors and ephrin ligands are membrane-binding proteins and the formation of the Eph/ephrin complex initiates bidirectional signals. The activated receptor tyrosine kinase transduces intracellular signals ("forward" signaling), while the ligand acts as a scaffold to transmit signals in its host cell ("reverse" signaling). The Eph receptor family comprises 14 members in humans and other mammals and is divided into two subfamilies based on sequence conservation and ligand binding affinity: EphA (EphA1-EphA8 and EphA10) and EphB (EphB1-EphB4 and EphB6). Eph receptors are activated when bound to membrane-combined ephrin ligands. A total of nine EphA receptors preferentially bind to five glycosylphosphatidylinositol-anchored ephrin-A ligands (ephrin-A1-A5). In addition, five EphB receptors possess high-affinity binding domains to three transmembrane ephrin-B (ephrin-B1-B3) ligands [37]. EphA4 and EphB2 are exceptions, which can bind to both A-type and most B-type ligands [16]. RhoA and its downstream effector, ROCK, are one group of key components of ephrin reverse signaling [33]. ROCK is a serine/threonine kinase that is expressed as two homologs, ROCK1 and ROCK2. These two isoforms share similar structure and function, but are expressed at different levels in different organs. ROCK1 is highly expressed in liver, lung, testes, blood, and the immune system, whereas ROCK2 is the dominant form in the brain and muscles [11, 24]. Activation of RhoA/ROCK2 pathway appears to be instrumental for the modulation of the microglial phenotype [27, 38]. Here, we found that inhibition of neuronal EphA4 leads to decreased expression of activated RhoA and ROCK2, which is believed to be responsible for alternative activation of microglia [1, 28, 34].

We cannot rule out the possibility that EphA4 shRNA exerts its influence on neuronal protection through other approaches, such as suppression of EphA4 forward signaling. Besides, previous findings showed that activation of EphA forward signaling can promotes Ephexin-dependent RhoA/ROCK pathway [30]. However, RhoA/ROCK activated by EphA forward signaling has been proved to mainly function through manipulating cytoskeletal dynamics [25, 29, 30]. So, it is conceivable that alternative activation of microglia mediated by EphA4/ephrin signaling between neuron and microglia is the major neuroprotective mechanism that underlines EphA4 shRNA treatment after OGD/R.

In conclusion, application of EphA4 shRNA silencing neuronal EphA4 reduced inflammatory injury through shifting microglia M1 phenotype to M2 phenotype, and providing neuroprotective environment *via* RhoA/ROCK2 signaling after OGD/R. A better understanding of the cellular and molecular mechanisms regulating EphA4/ephrin signaling may help researchers identify potential targets and develop clinical therapies for various neurological diseases.

FUNDING INFORMATION

This work was partly financially supported by the Fujian Provincial Natural Science Foundation (Grant nos. 2017J05123 and 2018J01175); Startup Fund for Scientific Research, Fujian Medical University (Grant No. 2016QH067); Young and Middle-aged Backbone Key Research Project of the National Health and Family Planning Commission of Fujian Province (Grant nos. 2017-ZQN-46 and 2018-ZQN-48); and the National Natural Science Foundation of China (Grant no. 81802492).

COMPLIANCE WITH ETHICAL STANDARDS

Conflict of Interest. The authors declare that they have no conflict of interest.

REFERENCES

1. Borrajo, A., A.I. Rodriguez-Perez, B. Villar-Cheda, M.J. Guerra, and J.L. Labandeira-Garcia. 2014. Inhibition of the microglial response is essential for the neuroprotective effects of Rho-kinase inhibitors on MPTP-induced dopaminergic cell death. *Neuropharmacology* 85: 1–8. https://doi.org/10.1016/j.neuropharm.2014.05.021.
2. Carmona, M.A., K.K. Murai, L. Wang, A.J. Roberts, and E.B. Pasquale. 2009. Glial ephrin-A3 regulates hippocampal dendritic

spine morphology and glutamate transport. *Proceedings of the National Academy of Sciences of the United States of America* 106 (30): 12524–12529. https://doi.org/10.1073/pnas.0903328106.
3. Cherry, J.D., J.A. Olschowka, and M.K. O'Banion. 2014. Neuroinflammation and M2 microglia: the good, the bad, and the inflamed. *Journal of Neuroinflammation* 11: 98. https://doi.org/10.1186/1742-2094-11-98.
4. Corraliza, I.M., G. Soler, K. Eichmann, and M. Modolell. 1995. Arginase induction by suppressors of nitric oxide synthesis (IL-4, IL-10 and PGE2) in murine bone-marrow-derived macrophages. *Biochemical and Biophysical Research Communications* 206 (2): 667–673. https://doi.org/10.1006/bbrc.1995.1094.
5. Elbashir, S.M., J. Harborth, W. Lendeckel, A. Yalcin, K. Weber, and T. Tuschl. 2001. Duplexes of 21-nucleotide RNAs mediate RNA interference in cultured mammalian cells. *Nature* 411 (6836): 494–498. https://doi.org/10.1038/35078107.
6. Fan, R., B. Enkhjargal, R. Camara, F. Yan, L. Gong, J. Tang ShengtaoYao, Y. Chen, and J.H. Zhang. 2017. Critical role of EphA4 in early brain injury after subarachnoid hemorrhage in rat. *Experimental Neurology* 296: 41–48. https://doi.org/10.1016/j.expneurol.2017.07.003.
7. Fang, Q., A. Strand, W. Law, V.M. Faca, M.P. Fitzgibbon, N. Hamel, B. Houle, X. Liu, D.H. May, G. Poschmann, L. Roy, K. Stühler, W. Ying, J. Zhang, Z. Zheng, J.J.M. Bergeron, S. Hanash, F. He, B.R. Leavitt, H.E. Meyer, X. Qian, and M.W. McIntosh. 2009. Brain-specific proteins decline in the cerebrospinal fluid of humans with Huntington disease. *Molecular & Cellular Proteomics* 8 (3): 451–466. https://doi.org/10.1074/mcp.M800231-MCP200.
8. Filosa, A., S. Paixao, S.D. Honsek, M.A. Carmona, L. Becker, B. Feddersen, L. Gaitanos, et al. 2009. Neuron-glia communication via EphA4/ephrin-A3 modulates LTP through glial glutamate transport. *Nature Neuroscience* 12 (10): 1285–1292. https://doi.org/10.1038/nn.2394.
9. Fu, A.K., K.W. Hung, H. Huang, S. Gu, Y. Shen, E.Y. Cheng, F.C. Ip, X. Huang, W.Y. Fu, and N.Y. Ip. 2014. Blockade of EphA4 signaling ameliorates hippocampal synaptic dysfunctions in mouse models of Alzheimer's disease. *Proceedings of the National Academy of Sciences of the United States of America* 111 (27): 9959–9964. https://doi.org/10.1073/pnas.1405803111.
10. Gingras, M., V. Gagnon, S. Minotti, H.D. Durham, and F. Berthod. 2007. Optimized protocols for isolation of primary motor neurons, astrocytes and microglia from embryonic mouse spinal cord. *Journal of Neuroscience Methods* 163 (1): 111–118. https://doi.org/10.1016/j.jneumeth.2007.02.024.
11. Hashimoto, R., Y. Nakamura, H. Kosako, M. Amano, K. Kaibuchi, M. Inagaki, and M. Takeda. 1999. Distribution of Rho-kinase in the bovine brain. *Biochemical and Biophysical Research Communications* 263 (2): 575–579. https://doi.org/10.1006/bbrc.1999.1409.
12. He, G.Q., W.M. Xu, J.F. Li, S.S. Li, B. Liu, X.D. Tan, and C.Q. Li. 2015. Huwe1 interacts with Gadd45b under oxygen-glucose deprivation and reperfusion injury in primary rat cortical neuronal cells. *Molecular Brain* 8: 88. https://doi.org/10.1186/s13041-015-0178-y.
13. Hu, X., R.K. Leak, Y. Shi, J. Suenaga, Y. Gao, P. Zheng, and J. Chen. 2015. Microglial and macrophage polarization-new prospects for brain repair. *Nature Reviews. Neurology* 11 (1): 56–64. https://doi.org/10.1038/nrneurol.2014.207.
14. Hu, X., P. Li, Y. Guo, H. Wang, R.K. Leak, S. Chen, Y. Gao, and J. Chen. 2012. Microglia/macrophage polarization dynamics reveal novel mechanism of injury expansion after focal cerebral ischemia. *Stroke* 43 (11): 3063–3070. https://doi.org/10.1161/STROKEAHA.112.659656.
15. Kemmerling, N., P. Wunderlich, S. Theil, B. Linnartz-Gerlach, N. Hersch, B. Hoffmann, M.T. Heneka, B. de Strooper, H. Neumann, and J. Walter. 2017. Intramembranous processing by gamma-secretase regulates reverse signaling of ephrin-B2 in migration of microglia. *Glia* 65 (7): 1103–1118. https://doi.org/10.1002/glia.23147.
16. Klein, R. 2009. Bidirectional modulation of synaptic functions by Eph/ephrin signaling. *Nature Neuroscience* 12 (1): 15–20. https://doi.org/10.1038/nn.2231.
17. Lemmens, R., T. Jaspers, W. Robberecht, and V.N. Thijs. 2013. Modifying expression of EphA4 and its downstream targets improves functional recovery after stroke. *Human Molecular Genetics* 22 (11): 2214–2220. https://doi.org/10.1093/hmg/ddt073.
18. Li, J., N. Liu, Y. Wang, R. Wang, D. Guo, and C. Zhang. 2012. Inhibition of EphA4 signaling after ischemia-reperfusion reduces apoptosis of CA1 pyramidal neurons. *Neuroscience Letters* 518 (2): 92–95. https://doi.org/10.1016/j.neulet.2012.04.060.
19. Livak, K.J., and T.D. Schmittgen. 2001. Analysis of relative gene expression data using real-time quantitative PCR and the 2(-Delta Delta C(T)) method. *Methods* 25 (4): 402–408. https://doi.org/10.1006/meth.2001.1262.
20. Ma, Y., J. Wang, Y. Wang, and G.Y. Yang. 2017. The biphasic function of microglia in ischemic stroke. *Progress in Neurobiology* 157: 247–272. https://doi.org/10.1016/j.pneurobio.2016.01.005.
21. Morris, S.M., Jr. 2007. Arginine metabolism: boundaries of our knowledge. *The Journal of Nutrition* 137 (6 Suppl 2): 1602S–1609S. https://doi.org/10.1093/jn/137.6.1602S.
22. Munro, K.M., V.M. Perreau, and A.M. Turnley. 2012. Differential gene expression in the EphA4 knockout spinal cord and analysis of the inflammatory response following spinal cord injury. *PLoS One* 7 (5): e37635. https://doi.org/10.1371/journal.pone.0037635.
23. Murai, K.K., L.N. Nguyen, F. Irie, Y. Yamaguchi, and E.B. Pasquale. 2003. Control of hippocampal dendritic spine morphology through ephrin-A3/EphA4 signaling. *Nature Neuroscience* 6 (2): 153–160. https://doi.org/10.1038/nn994.
24. Nakagawa, O., K. Fujisawa, T. Ishizaki, Y. Saito, K. Nakao, and S. Narumiya. 1996. ROCK-I and ROCK-II, two isoforms of Rho-associated coiled-coil forming protein serine/threonine kinase in mice. *FEBS Letters* 392 (2): 189–193.
25. Noren, N.K., and E.B. Pasquale. 2004. Eph receptor-ephrin bidirectional signals that target Ras and Rho proteins. *Cellular Signalling* 16 (6): 655–666. https://doi.org/10.1016/j.cellsig.2003.10.006.
26. Qin, H., R. Noberini, X. Huan, J. Shi, E.B. Pasquale, and J. Song. 2010. Structural characterization of the EphA4-Ephrin-B2 complex reveals new features enabling Eph-ephrin binding promiscuity. *The Journal of Biological Chemistry* 285 (1): 644–654. https://doi.org/10.1074/jbc.M109.064824.
27. Roser, A.E., L. Tonges, and P. Lingor. 2017. Modulation of microglial activity by Rho-kinase (ROCK) inhibition as therapeutic strategy in Parkinson's disease and amyotrophic lateral sclerosis. *Frontiers in Aging Neuroscience* 9: 94. https://doi.org/10.3389/fnagi.2017.00094.
28. Scheiblich, H., and G. Bicker. 2017. Regulation of microglial phagocytosis by RhoA/ROCK-inhibiting drugs. *Cellular and Molecular Neurobiology* 37 (3): 461–473. https://doi.org/10.1007/s10571-016-0379-7.
29. Schmucker, D., and S.L. Zipursky. 2001. Signaling downstream of Eph receptors and ephrin ligands. *Cell* 105 (6): 701–704.
30. Shamah, S.M., M.Z. Lin, J.L. Goldberg, S. Estrach, M. Sahin, L. Hu, M. Bazalakova, R.L. Neve, G. Corfas, A. Debant, and M.E. Greenberg. 2001. EphA receptors regulate growth cone dynamics through the novel guanine nucleotide exchange factor ephexin. *Cell* 105 (2): 233–244.
31. Shu, Y., B. Xiao, Q. Wu, T. Liu, Y. Du, H. Tang, S. Chen, L. Feng, L. Long, and Y. Li. 2016. The Ephrin-A5/EphA4 interaction modulates

neurogenesis and angiogenesis by the p-Akt and p-ERK pathways in a mouse model of TLE. *Molecular Neurobiology* 53 (1): 561–576. https://doi.org/10.1007/s12035-014-9020-2.

32. Takahashi, I., Y. Hama, M. Matsushima, M. Hirotani, T. Kano, H. Hohzen, I. Yabe, J. Utsumi, and H. Sasaki. 2015. Identification of plasma microRNAs as a biomarker of sporadic amyotrophic lateral sclerosis. *Molecular Brain* 8 (1): 67. https://doi.org/10.1186/s13041-015-0161-7.
33. Takeuchi, S., H. Katoh, and M. Negishi. 2015. Eph/ephrin reverse signalling induces axonal retraction through RhoA/ROCK pathway. *Journal of Biochemistry* 158 (3): 245–252. https://doi.org/10.1093/jb/mvv042.
34. Tatsumi, E., H. Yamanaka, K. Kobayashi, H. Yagi, M. Sakagami, and K. Noguchi. 2015. RhoA/ROCK pathway mediates p38 MAPK activation and morphological changes downstream of P2Y12/13 receptors in spinal microglia in neuropathic pain. *Glia* 63 (2): 216–228. https://doi.org/10.1002/glia.22745.
35. Xiao, H., Q. Huang, J.Q. Wang, Q.Q. Deng, and W.P. Gu. 2016. Effect of ephrin-B2 on the expressions of angiopoietin-1 and -2 after focal cerebral ischemia/reperfusion. *Neural Regeneration Research* 11 (11): 1784–1789. https://doi.org/10.4103/1673-5374.194723.
36. Yang, J., X. Luo, X. Huang, Q. Ning, M. Xie, and W. Wang. 2014. Ephrin-A3 reverse signaling regulates hippocampal neuronal damage and astrocytic glutamate transport after transient global ischemia. *Journal of Neurochemistry* 131 (3): 383–394. https://doi.org/10.1111/jnc.12819.
37. Yang, J.S., H.X. Wei, P.P. Chen, and G. Wu. 2018. Roles of Eph/ephrin bidirectional signaling in central nervous system injury and recovery. *Experimental and Therapeutic Medicine* 15 (3): 2219–2227. https://doi.org/10.3892/etm.2018.5702.
38. Zhang, H., Y. Li, J. Yu, M. Guo, J. Meng, C. Liu, Y. Xie, L. Feng, B. Xiao, and C. Ma. 2013. Rho kinase inhibitor fasudil regulates microglia polarization and function. *Neuroimmunomodulation* 20 (6): 313–322. https://doi.org/10.1159/000351221.
39. Zujovic, V., and V. Taupin. 2003. Use of cocultured cell systems to elucidate chemokine-dependent neuronal/microglial interactions: control of microglial activation. *Methods* 29 (4): 345–350.